Available online at www.sciencedirect.com
SCIENCE DIRECT®
PERGAMON
International Journal of Heat and Mass Transfer 46 (2003) 5045–5057
International Journal of HEAT and MASS TRANSFER
www.elsevier.com/locate/ijhmt

The characteristics of turbulent flow and convection in concentric circular annuli. Part I: flow

Masayuki Kaneda [a], Bo Yu [a], Hiroyuki Ozoe [a], Stuart W. Churchill [b,*]

[a] *Institute of Advanced Material Study, Kyushu University, Kasuga, Fukuoka 816, Japan*
[b] *Department of Chemical and Biomolecular Engineering, University of Pennsylvania, 311A Towne Building, 220 South 33rd Street, Philadelphia, PA 19104, USA*

Received 23 December 2002; received in revised form 24 June 2003

Abstract

New, more accurate values for the time-averaged velocity distribution and the mixed-mean velocity (and thereby the friction factor) were obtained for fully developed turbulent flow in annuli by numerical integration of the equations of conservation using a theoretically based correlating equation for the turbulent shear stress. These computed values are represented almost exactly by simple algebraic equations that may be considered to be predictive rather than correlative because they have a theoretical structure, are virtually free from empiricism, and are not based on the calculated values. These predictive expressions agree closely with the most reliable experimental data within their scatter.

1. Introduction

Despite many investigations, the existing computational and experimental results for turbulent flow and convection in annuli are quite incomplete and uncertain. The results reported here for flow were undertaken primarily to provide a basis for improved predictions of convection. However the characteristics of the flow proved to be of direct interest because of their complete scope. These values were obtained by numerical integration of the equations of conservation using a theoretically based correlating equation for the turbulent shear stress. The effect of the small degree of empiricism associated with this form of modeling has previously been shown to be a negligible source of error in predictions for round tubes and parallel-plate channels (see, [1,2]).

The primary practical interest in turbulent flow in a concentric circular annulus is in connection with convective heat transfer in the outer passage of a double-pipe heat exchanger. Because of the non-linear radial variation of the total shear stress within the fluid, the analysis of flow in an annulus is considerably more complex than in a round tube or parallel-plate channel in the laminar as well as in the turbulent regime. As the aspect ratio (inner diameter/outer diameter) increases toward unity, the velocity distribution and the friction factor approach those for a parallel-plate channel in turbulent as well as in laminar flow. As the aspect ratio decreases toward zero, the velocity distribution approaches that for a round tube but never quite attains it because the velocity remains zero and the velocity gradient finite at the inner wall. Even so, the friction factor approaches that for a round tube, again in both laminar and turbulent flow.

As a consequence of its relative complexity, the behavior of both flow and convective heat transfer in an annulus in the turbulent regime is as yet incompletely characterized and generalized either experimentally or theoretically. The objective of this investigation has been to improve upon that description in a quantitative sense by a combination of theoretical and correlative methodologies. The specific plan has been, first to devise improved, theoretically based correlating equations for the turbulent shear stress distribution, second to utilize such expressions to calculate the total shear stress

* Corresponding author. Tel.: +1-215-898-5579; fax: +1-215-573-2093.
E-mail address: churchil@seas.upenn.edu (S.W. Churchill).

0017-9310/$ - see front matter © 2003 Elsevier Ltd. All rights reserved.
doi:10.1016/S0017-9310(03)00365-X

distribution, the time–mean velocity distribution, and the time- and space–mean velocity, third to utilize these latter numerical values and the structure of the correlating equations for the turbulent shear stress to develop a generalized predictive equation for each of these quantities, fourth to utilize the computed values for flow and these predictive and correlative expressions, together with a correlative or predictive equation for the turbulent Prandtl number, to calculate numerical values for the heat flux distribution, the time-averaged temperature distribution, and the mixed-mean temperature, and fifth to develop generalized correlating equations for the Nusselt number as a function of the Reynolds number, the Prandtl number, the aspect ratio, and the mode of heating at the surfaces. This mission has been accomplished in large part. The procedure and results for flow are reported herein. Those for heat transfer will follow in Parts II–IV.

Lorenz [3] in 1937 discovered experimentally that in turbulent flow the location of the maximum in the time–mean velocity distribution in an annulus differs measurably from that for laminar flow. Kjellström and Hedberg [4] in 1966 derived integral expressions involving the local turbulent shear stress from which it may be inferred that the location of the maximum in the velocity differs from the location of the zero in the total shear stress as well as from their common location in laminar flow. They were unable to confirm experimentally the difference in location between the maximum in the velocity distribution and the zero in the total shear stress for a smooth annulus, but did succeed for an annulus with a roughened inner surface, for which the difference in locations is magnified. Finally in 1972, Lawn and Elliott [5] confirmed experimentally the non-coincidence for smooth annuli.

Because, as illustrated schematically in Fig. 1, the total shear stress is finite at the location where the velocity is a maximum and its gradient is zero, the eddy viscosity and the mixing length are both unbounded at that point. Also, because the sign of the velocity gradient changes at that point while that of the total shear stress does not, the eddy viscosity and the mixing length are negative over a small adjacent finite range of the radius. This "anomalous" behavior occurs for all aspect ratios and all Reynolds numbers in the fully turbulent regime ($a_2^+ - a_1^+ \geqslant 300$). As a consequence of overlooking this aspect of behavior, no doubt in part because of the somewhat obscure publications in which the work of Lorenz and of Kjellström and Hedberg was reported, almost all of the theoretical and semi-theoretical predictive expressions for the time–mean velocity distribution, friction factor, and Nusselt number in the current literature are subject to unidentifiable but possibly significant error. The only exceptions appear to be the predictions of flow by Hanjalić and Launder [6] using a k–ε–$\overline{u'v'}$ model, by Kawamura et al. [7], and Satake and Kawamura [8] using large-eddy simulation (LES), and by Chung et al. [9] using direct numerical simulation (DNS). All of these latter methodologies, except for DNS, for which the calculations are restricted to rates of flow barely above the minimum for fully developed turbulence, invoke the eddy viscosity but avoid its use in the region of non-coincidence. They also invoke empirical wall-functions.

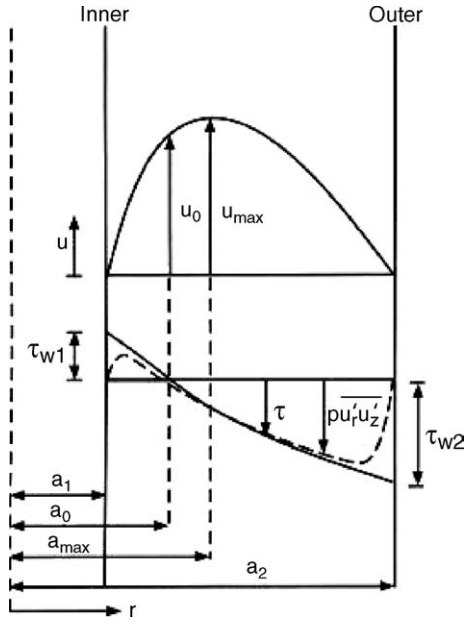

Fig. 1. Schematic representation of characteristics of turbulent flow in annuli.

Because prior work on turbulent flow and convection in annuli was recently reviewed by Churchill [10], and because most of the prior predictive results are highly uncertain owing to the failure to account for the displacement of the maximum in the velocity from that for laminar flow and/or from the zero in the total shear stress, a comprehensive review does not appear to be necessary here. Of course, all directly relevant prior work is noted in context.

2. Mathematical structure for representation of turbulent flow

The time-averaged once-integrated force–momentum balance for the stationary, fully developed a fluid of invariant physical properties in a concentric, circular annulus may be written as

$$\tau = \mu \frac{\mathrm{d}u}{\mathrm{d}r} - \rho \overline{u_r' u_z'} \tag{1}$$

Here τ is the total, time-averaged shear stress in the z-direction imposed on the fluid at r, the radial distance from the axis, by the fluid at greater r, μ, and ρ are the

viscosity and density of the fluid, u is the local, time–mean velocity, and $\overline{u'_r v'_z}$ is the time-averaged product of the components of the fluctuating velocity. Although, in the turbulent regime, a slight radial gradient exists in the time-averaged pressure, the axial gradient, $-\mathrm{d}p/\mathrm{d}z$, is independent of radius, allowing the following force balance to be constructed in terms of a_0, the radial location of the zero in the total shear stress:

$$\tau = \left(-\frac{\mathrm{d}p}{\mathrm{d}z}\right)\left(\frac{a_0^2 - r^2}{2r}\right) \tag{2}$$

Eqs. (1) and (2) are applicable for the entire cross-section, that is, from the inner radius a_1 to the outer radius a_2. As indicated in Fig. 1, τ, as defined by Eq. (2), is positive for $r < a_0$ and negative for $r > a_0$. However, for convenience, the shear stresses on the inner and outer surfaces are defined as $\tau_{w1} = \tau_{r=a_1}$ and $\tau_{w2} = -\tau_{r=a_2}$, respectively, and are thereby both positive.

Eq. (1) may be re-expressed in the following dimensionless form proposed by Churchill and Chan [11]:

$$\frac{\tau}{\tau_w} = \frac{\mathrm{d}u^+}{\mathrm{d}y^+} + (\overline{u'v'})^+ \tag{3}$$

Here, $(\overline{u'v'})^+ = -\rho\overline{u'v'}/\tau_w$, $u^+ = u(\rho/\tau_w)^{1/2}$, $y = r - a$, the radial distance from the inner wall, and $y^+ = y(\rho\tau_w)^{1/2}/\mu$. Churchill [12] found that $(\overline{u'v'})^{++} = -\rho\overline{u'v'}/\tau$ was more tractable than $(\overline{u'v'})^+$ for round tubes and parallel plates, but in an annulus this quantity shares the singularity of the eddy viscosity and the mixing length, and therefore is not utilized here.

Several relationships that prove to be useful in what follows may be inferred from Eq. (2), namely

$$\frac{\tau}{\tau_{w1}} = \frac{a_1}{r}\left(\frac{a_0^2 - r^2}{a_0^2 - a_1^2}\right) \tag{4}$$

$$\tau_{w1} = \left(-\frac{\mathrm{d}p}{\mathrm{d}z}\right)\left(\frac{a_0^2 - a_1^2}{2a_1}\right) \tag{5}$$

$$\tau_{w2} = \left(-\frac{\mathrm{d}p}{\mathrm{d}z}\right)\left(\frac{a_2^2 - a_0^2}{2a_2}\right) \tag{6}$$

and

$$\frac{\tau_{w1}}{\tau_{w2}} = \frac{a_2}{a_1}\left(\frac{a_0^2 - a_1^2}{a_2^2 - a_0^2}\right) \tag{7}$$

Eqs. (1)–(7) are exact within the commonplace restrictions placed on the flow and are applicable for all conditions. However, in order to determine $u\{r\}$ and u_m for a specified value of $-\mathrm{d}p/\mathrm{d}z$ or w, a specified fluid (characterized by μ and ρ), and specified values of a_1 and a_2, empirical relationships are required for $(\overline{u'v'})^+$, a_0, and $a_{\max}$. Here, w is the mass rate of flow, and $a_{\max}$ is the radial location of the maximum in the velocity profile.

Kays and Leung [13] correlated experimental data of various investigations for the location of the maximum in the velocity distribution in the turbulent regime with the empirical expression

$$\frac{a_{\max} - a_1}{a_2 - a_{\max}} = \left(\frac{a_1}{a_2}\right)^{0.343} \tag{8}$$

Rehme [14] similarly correlated his own experimental data as well as that of others for the location of the zero in the total shear stress for $Re = 10^5$ with the expression

$$\frac{a_0 - a_1}{a_2 - a_0} = \left(\frac{a_1}{a_2}\right)^{0.386} \tag{9}$$

These two empirical expressions, both of which are implied to be independent of the rate of flow, are utilized herein. The experimental evidence concerning this implicit postulate of independence from the rate of flow is limited, but some indirect support is provided by the independence from flow of the exact theoretical expression for $a_{\max}$ $(= a_0)$ for the laminar regime, namely,

$$\left(\frac{a_{\max}}{a_1}\right)^2 = \frac{[(a_2/a_1)^2 - 1]}{\ln(a_2/a_1)^2} \tag{10}$$

The numerical results that are presented herein for flow and convection are subject to some unknown, but presumably fairly limited, error by virtue of their dependence on Eqs. (8) and (9). Owing to the severe limitation of DNS in terms of the range of flow, and the uncertainty of all other theoretical models, the general prediction of a_0 and $a_{\max}$ for turbulent flow from first principles is not feasible at present. The determination of improved values or expressions for these two quantities may eventually provide the basis for updating the results presented herein for the turbulent shear stress distribution, the time–mean velocity distribution and the friction factor, but, as shown herein by means of using Eq. (10) in place of Eqs. (8) and (9) in test calculations, such improvements would be expected to be minimal.

3. Correlating equations for the turbulent shear stress

The same general procedure and the same general form as used by Churchill and Chan [11] to develop a correlating equation for $(\overline{u'v'})^+$ for a round tube and a parallel-plate channel was adapted for annuli, but separate expressions were necessarily devised for the inner region, $a_1 \leqslant r \leqslant a_{\max}$, and the outer region, $a_{\max} \leqslant r \leqslant a_2$. Both of these correlating equations have the overall form

$$[(\overline{u'v'})^+]^n = [(\overline{u'v'})_0^+]^n + [(\overline{u'v'})_\infty^+]^n \tag{11}$$

with an arbitrary combining exponent n of $-8/7$. On the basis of direct numerical simulations for parallel-plate channels, the following asymptotic expression for small values of y^+ is presumed to be applicable for all shear

flows, including the inner and outer regions of an annulus:

$$(\overline{u'v'})_0^+ = 0.7\left(\frac{y^+}{10}\right)^3\left(\frac{\tau}{\tau_\omega}\right) \tag{12}$$

On the other hand, while an equivalent general asymptotic expression for $(\overline{u'v'})_\infty^+$ has not been derived directly, one can be constructed from the following speculative expression devised by Churchill and Chan [11] for the time–mean velocity distribution in the turbulent core of a round tube:

$$u^+ = A + B\ln\{y^+\} + C\left(\frac{y^+}{a^+}\right)^2 - \frac{(2B+C)}{3}\left(\frac{y^+}{a^+}\right)^3 \tag{13}$$

Here, A, B, and C are arbitrary constants, and $a^+ = a(\rho\tau_w)^{1/2}/\mu$. Eq. (13) reduces to the generally accepted semi-logarithmic expression for "the turbulent core near the wall" for $30 \leqslant y^+ \leqslant 0.1a^+$ and conforms to the necessary condition of $\mathrm{d}u^+/\mathrm{d}y^+ = 0$ at $y^+ = a^+$, as well as to the speculative asymptote $u_c^+ - u^+ = E(1-y/a)^2$ for $y^+ \to a^+$. Here u_c is the velocity at the centerline. On the basis of Eq. (3), it follows from Eq. (13) that

$$(\overline{u'v'})_\infty^+ = \frac{\tau}{\tau_\omega} - \left(1-\frac{y^+}{a^+}\right)\left[\frac{B}{y^+} + \frac{B}{a^+}\left\{1+\left(1+\frac{2C}{B}\right)\frac{y^+}{a^+}\right\}\right] \tag{14}$$

Eqs. (13) and (14) are directly applicable for parallel-plate channels if a^+ is simply replaced by $b^+ = b(\rho\tau_w)^{1/2}/\mu$, where b is the half-width of the channel. They might therefore be expected to be applicable for both the inner and outer regions for the "intermediate" case of an annulus.

When Eqs. (12) and (14) are specialized for the inner region of an annulus, the dimensionless distance from the wall, y^+, is replaced by $r^+ - a_1^+$, the radius, a^+, by $a_{\max}^+ - a_1^+$, the shear stress at the wall, τ_w, by $\tau_{\omega 1}$, and the shear stress ratio τ/τ_ω by $\frac{a_1}{r}\left(\frac{a_0^2-r^2}{a_0^2-a_1^2}\right)$, resulting in

$$(\overline{u'v'})_0^+ = 0.7\left(\frac{r^+-a_1^+}{10}\right)^3\left(\frac{a_1}{r}\right)\left(\frac{a_0^2-r^2}{a_0^2-a_1^2}\right) \tag{15}$$

and

$$(\overline{u'v'})_\infty^+ = \frac{a_1}{r}\left(\frac{a_0^2-r^2}{a_0^2-a_1^2}\right) - \left(\frac{a_{\max}-r}{a_{\max}-a_1}\right) \times\left\{\frac{B}{(r^+-a_1^+)} + \frac{B}{(a_{\max}^+-a_1^+)} \times\left[1+\left(1+\frac{2C}{B}\right)\left(\frac{r-a_1}{a_{\max}-a_1}\right)\right]\right\} \tag{16}$$

Here, $(\overline{u'v'})^+$, r^+, a_1^+ and $a_{\max}^+$ are normalized with respect to $\tau_{\omega 1}$.

For the outer region, Eqs. (11) and (13) are directly applicable in terms of $\tau/\tau_\omega = \tau/\tau_{\omega 2}$, $(\overline{u'v'})^+$, $y^+ = a_2^+ - r^+$, and $a^+ = a_2^+ - a_{\max}^+$, all normalized in terms of τ_{w2}. However, in order to be compatible numerically with $(\overline{u'v'})^+$ for the inner region, it is convenient to re-normalize these two equations in terms of $\tau_{\omega 1}$. The result is

$$\begin{aligned}(\overline{u'v'})_0^+ &= 0.7\left(\frac{a_2^+-r^+}{10}\right)^3\left(\frac{\tau}{\tau_{\omega 1}}\right)\left(\frac{\tau_{\omega 2}}{\tau_{\omega 1}}\right)^{3/2}\\ &= 0.7\left(\frac{a_2^+-r^+}{10}\right)^3\left(\frac{a_1}{r}\right)\left(\frac{a_0^2-r^2}{a_0^2-a_1^2}\right) \times\left(\frac{a_2^2-a_0^2}{a_0^2-a_1^2}\right)^{3/2}\left(\frac{a_1}{a_2}\right)^{3/2}\end{aligned} \tag{17}$$

and

$$(\overline{u'v'})_\infty^+ = \frac{a_1}{r}\left(\frac{a_0^2-r^2}{a_0^2-a_1^2}\right) - \left(\frac{a_1}{a_2}\right)^{1/2}\left(\frac{a_2^2-a_0^2}{a_0^2-a_1^2}\right)^{1/2} \times\left(\frac{r-a_{\max}}{a_2-a_{\max}}\right)\left\{\frac{B}{a_2^+-r^+} + \frac{B}{a_2^+-a_{\max}^+} \times\left[1+\left(\frac{2C}{B}+1\right)\left(\frac{a_2-r}{a_2-a_{\max}}\right)\right]\right\} \tag{18}$$

Eqs. (16) and (18) give the same value of $(\overline{u'v'})^+$ at $r = a_{\max}$ for all conditions and all choices of the arbitrary coefficients.

The recent and presumably most accurate experimental data for the velocity distribution in a round tube, namely those of Zagarola [15], suggest that the values of the coefficients A, B, and C in Eq. (13) may depend slightly on the rate of flow, but that 6.13, 1/0.436, and 6.824, respectively, are reasonable mean values. On the basis of the analogy of MacLeod [16], these same values are presumed to be applicable for a parallel-plate channel. Accordingly they are speculated to be directly applicable for the outer region ($r > a_{\max}$) of an annulus. However, for the inner region ($r < a_{\max}$), a different value of C, designated as C', is proposed in order to force the expressions for the velocity distribution in the inner and outer regions to match at $r = a_{\max}$. That is, C' is evaluated as a function of a_1/a_2 and $a_2^+ - a_1^+$ from

$$\begin{aligned}&A + B\ln\{a_{\max}^+ - a_1^+\} + \frac{C'-B}{3}\\ &= \left(\frac{a_1}{a_2}\right)^{1/2}\left(\frac{a_2^2-a_0^2}{a_0^2-a_1^2}\right)^{1/2}\left[A + B\ln\left\{(a_2^+-a_{\max}^+) \times\left(\frac{a_1}{a_2}\right)^{1/2}\left(\frac{a_2^2-a_0^2}{a_0^2-a_1^2}\right)^{1/2}\right\} + \frac{C-B}{3}\right]\end{aligned} \tag{19}$$

4. Numerical evaluations

Numerical calculations were carried out for all of the dimensionless dependent variables for all combinations of $a_1/a_2 = 0.001$, 0.01, 0.05, 0.1, 0.2, 0.5, 0.8, 0.9, 0.95,

0.99 and 0.999 and $a_2^+ - a_1^+ = 150$, 500, 800, 1000, 2000, 5000, 10,000, 20,000, 50,000, 100,000, 200,000 and 500,000 but only representative values are presented herein in graphical and tabular form. Throughout the balance of the paper, the absence of an additional subscript on a_1^+, a_2^+, r^+, y^+, $(\overline{u'v'})^+$, u_1^+, u_2^+, u_m^+, etc. implies that the quantity is normalized with respect to τ_{w1}, while a subscript of $w2$ designates normalization with respect to τ_{w2}, and a subscript of wm designates normalization with respect to the mean shear stress on the two walls, namely $\tau_{wm} = (a_1\tau_{w1} + a_2\tau_{w2})/(a_1 + a_2)$. This latter quantity is of primary practical interest because of its direct relationship to the axial pressure gradient, namely

$$\tau_{wm} = \frac{1}{2}\left(-\frac{\mathrm{d}p}{\mathrm{d}z}\right)(a_2 + a_1) \tag{20}$$

5. Numerical results and predictive expressions

Values of τ_{w2}/τ_{w1}, $a_{\max}/a_1$ and a_0/a_1, as computed from Eqs. (7)–(9), respectively, as well as the corresponding values of $a_1\tau_{w1}/a_2\tau_{w2}$, and τ_{wm}/τ_{w2} are listed in Table 1. The value of τ_{w1}/τ_{w2} increases as that of a_1/a_2 decreases, but insufficiently to prevent $a_1\tau_{w1}/a_2\tau_{w2} \to 0$ as $a_1/a_2 \to 0$. The combined variations of a_0/a_1 and τ_{w2}/τ_{w1} result, somewhat surprisingly, in $\tau_{wm}/\tau_{w2} \cong 1$ for all conditions. One consequence is that the Fanning friction factor based on τ_{wm}, namely $f_{wm} = 2(a_1\tau_{w1} + a_2\tau_{w2})/(a_1 + a_2)/\rho(u_m)_{wm}^2 = 2/(u_m^+)_{wm}$, approaches that for a round tube, as $a_1/a_2 \to 0$.

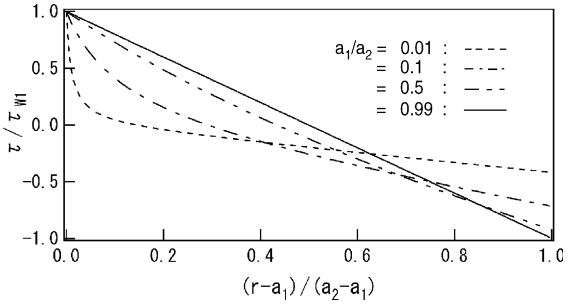

Fig. 2. Computed radial variation of the total shear stress within the fluid in turbulent flow through annuli of various aspect ratios.

Values of τ/τ_{w1} computed from Eqs. (7) and (9) are plotted in Fig. 2 versus the fractional distance across the annulus, namely $(r - a_1)/(a_2 - a_1)$, for four values of a_1/a_2. The variation is linear for $a_1/a_2 = 1$, but becomes very curved and steep near the inner surface and almost linear near the outer surface as $a_1/a_2 \to 0$.

Values C', as obtained from the numerical solution of Eq. (19), are listed in Table 2. As would be expected, they approach 6.824 as the values of $a_1/a_2 \to 1$ and of $a_2^+ - a_1^+ \to 0$. Values exceeding 6.824 are presumed to be a consequence of the failure to attain fully turbulent flow, and are shaded as an indication of probable unreliability. The unlisted values indicate unsatisfactory convergence of the calculations in some respect, not necessarily those for C'. The value of C', even when it differs significantly from 6.824, can be inferred from

Table 1
Characteristic ratios for annuli based on Eqs. (8) and (9)

a_1/a_2	0.01	0.1	0.2	0.5	0.8	0.9	0.95	0.99	0.999
$a_{\max}/a_1$	17.91	3.810	2.462	1.441	1.120	1.055	1.026	1.005	1.001
a_0/a_1	15.31	3.622	2.398	1.434	1.120	1.054	1.026	1.005	1.001
τ_{w2}/τ_{w1}	0.418	0.717	0.810	0.922	0.975	0.988	0.994	0.999	1.000
$(a_1\tau_{w1})/(a_2\tau_{w2})$	2.392×10^{-2}	0.140	0.247	0.542	0.821	0.911	0.956	0.991	0.999
τ_{wm}/τ_{w2}	1.014	1.036	1.039	1.028	1.011	1.006	1.003	1.001	1.000

Table 2
Compensatory coefficient C' for inner region based on Eqs. (8) and (9)

a_1/a_2	$a_2^+ - a_1^+$											
	50	500	800	1000	2000	5000	10,000	20,000	50,000	100,000	200,000	500,000
0.01		32.46	12.15	6.059	−1.227							
0.05	77.71	7.259	3.988	2.730	−0.373	−3.212	−5.120					
0.1	55.36	6.315	4.227	3.426	1.477	−0.305	−1.344	−2.265	−3.450	−4.545		
0.2	13.03	6.239	5.015	4.548	3.427	2.379	1.741	1.150	0.341	−0.374	−1.306	−3.296
0.5	8.914	6.564	6.119	5.955	5.545	5.153	4.893	4.635	4.227	3.788	3.120	1.424
0.8	7.465	6.740	6.600	6.548	6.417	6.279	6.188	6.069	5.839	5.528	4.974	3.411
0.9	7.123	6.781	6.716	6.690	6.626	6.558	6.489	6.414	6.227	5.948	5.423	3.893
0.95	6.969	6.802	6.769	6.755	6.722	6.680	6.634	6.575	6.403	6.141	5.626	4.114
0.99	6.851	6.817	6.810	6.805	6.795	6.776	6.747	6.694	6.539	6.287	5.785	4.282
0.999	6.825	6.820	6.819	6.817	6.812	6.796	6.773	6.721	6.570	6.320	5.820	4.318

either Eq. (13) or Eq. (22) to influence the calculated values of $u^+\{y^+\}$ only in the inner region near the maximum in the velocity, and even there only slightly, since the terms in which it occurs represent the perturbation from the semi-logarithmic dependence due to the wake.

Although $(\overline{u'v'})^+$ is the most important quantity involved in this analysis with respect to both flow and convection, it is unnecessary to present tabulated values because they may readily be evaluated on-line using Eqs. (11) and (14)–(18), together with the values of C' in Table 2. However, for illustration of the behavior, computed values of $(\overline{u'v'})^+$ are plotted in Fig. 3 for four values of a_1/a_2 and three values of $a_2^+ - a_1^+$. At both walls, the absolute value of $(\overline{u'v'})^+$ increases rapidly from zero to a maximum slightly less than unity, then decreases more slowly, and finally attains a nearly linear variation across the central part of the channel.

Values of u^+ for the inner region for $a_1/a_2 = 0.01$, 0.1, 0.5, and $a_2^+ - a_1^+ = 1000$, 10,000, and 100,000 as obtained by stepwise integration of Eq. (3), starting from the inner wall and using values of $(\overline{u'v'})^+$ computed as just described, are plotted versus y^+ in Fig. 4 for comparison with curves representing the adaption for annuli of the correlating equation of Churchill and Chan [11] for the velocity distribution in round tubes and parallel-plate channels, namely,

$$(u^+)^{-3} = (u_0^+)^{-3} + (u_\infty^+)^{-3} \tag{21}$$

Here u_∞^+, is given by Eq. (13) with the indicated values of A, B, and C' and u_0^+ is given by the following expression designed to correspond to Eq. (12) approximately, while avoiding a singularity in Eq. (21) as y^+ increases far above the range of validity of that asymptote:

$$u_0^+ = \frac{(y^+)^2}{1 + y^+ - \exp\{-1.75(y^+/10)^4\}} \tag{22}$$

The corresponding values of u_{wm}^+ for the outer region, as obtained by integrating from the outer wall, are plotted in Fig. 5. The separate starting points for the integration of Eq. (3) for the two regions were necessary to avoid, near the walls where the velocity is very small, the influence of accumulative errors due to discretization. No discrepancies are apparent visually in Figs. 4 and 5 between the values obtained by integration, as represented by the discrete symbols, and the curves representing Eq. (21) although minor ones must exist owing the approximation introduced by the use of Eq. (22) for u_0^+ and by the discordance between the interpolation for $(\overline{u'v'})^+$ with a combining exponent of −8/7, and that for u^+ with a combining exponent of −3. Such a good representation is a significant achievement because it allows the calculation of accurate values of u^+ from an algebraic equation for any set of values of a_1/a_2 and $a_2^+ - a_1^+$. This algebraic expression also expedites comparisons with experimental data, which are typically determined for odd values of both a_1/a_2 and $a_2^+ - a_1^+$.

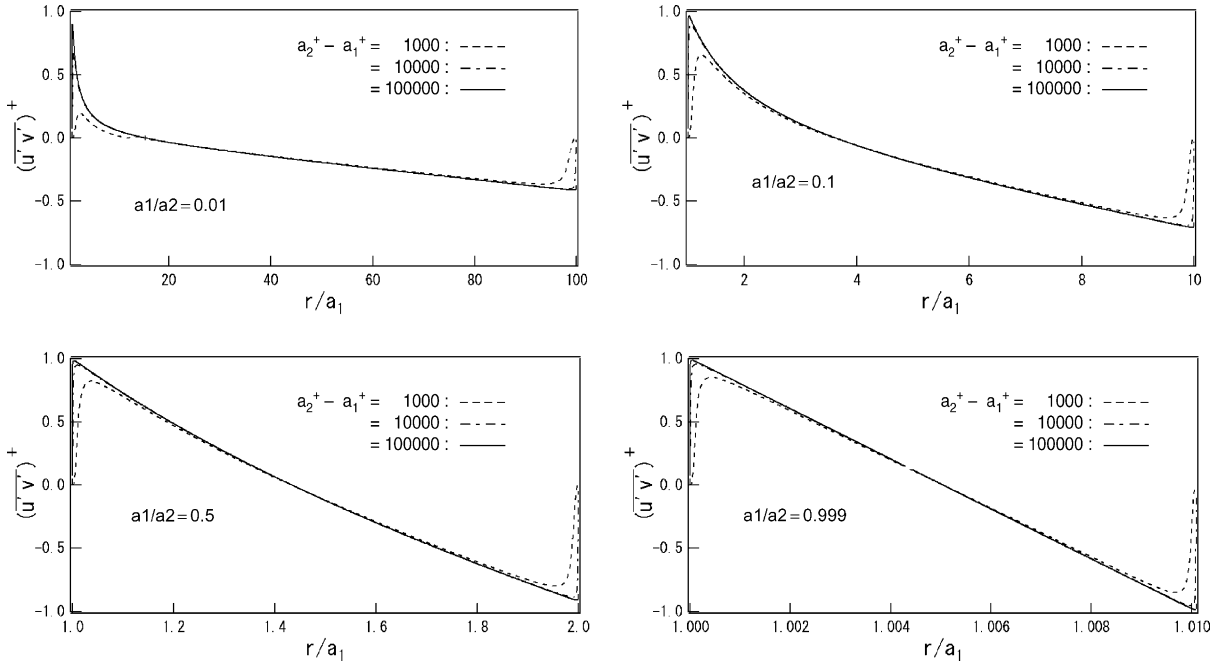

Fig. 3. Computed radial variation of the turbulent shear stress.

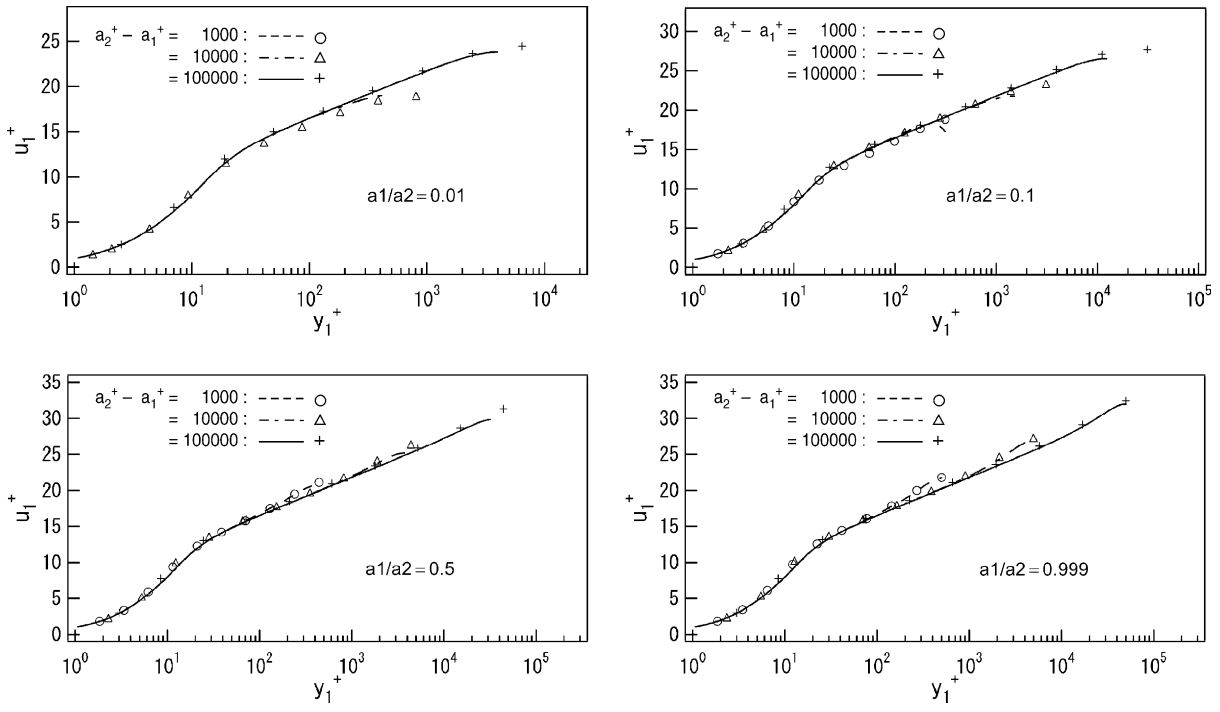

Fig. 4. Comparison of predictive expression for $u^+\{y^+\}$ in the inner region with computed values.

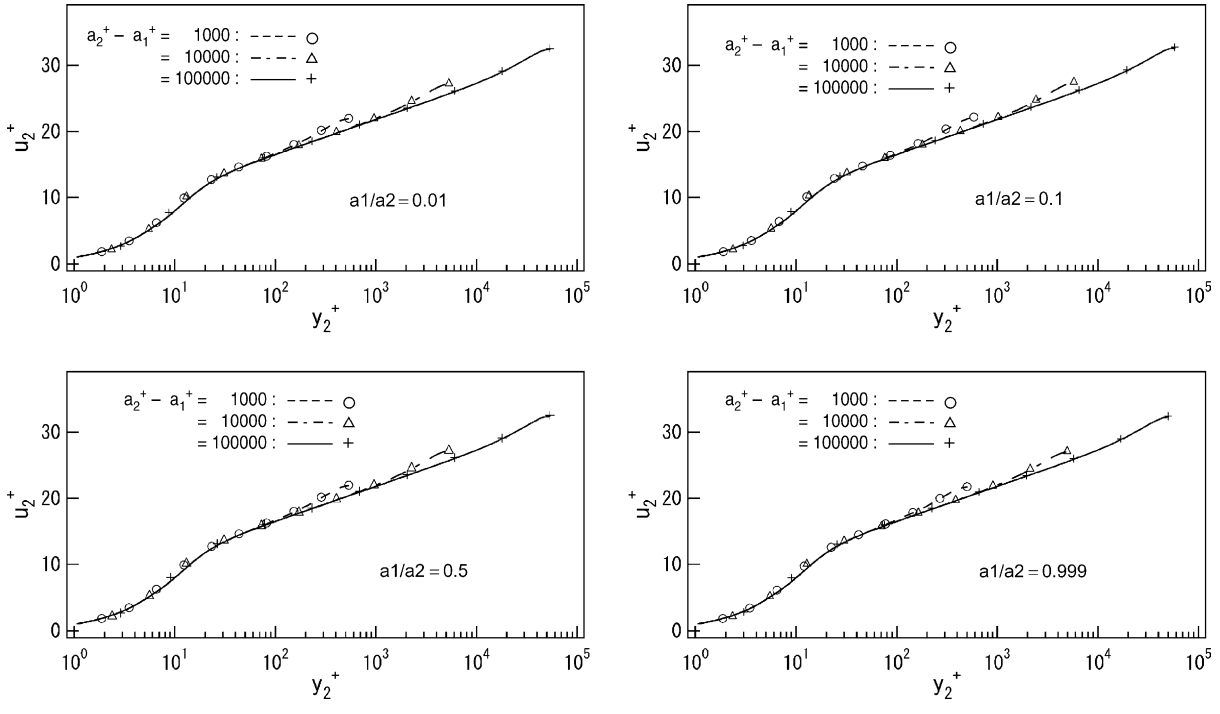

Fig. 5. Comparison of predictive expression for $u^+\{y^+\}$ in the outer region with computed values.

The computed values of u^+, as represented by Eq. (21), are compared with the experimental data of Rehme [14] in Figs. 6 and 7 for the inner and outer regions respectively. The agreement is generally within the scatter

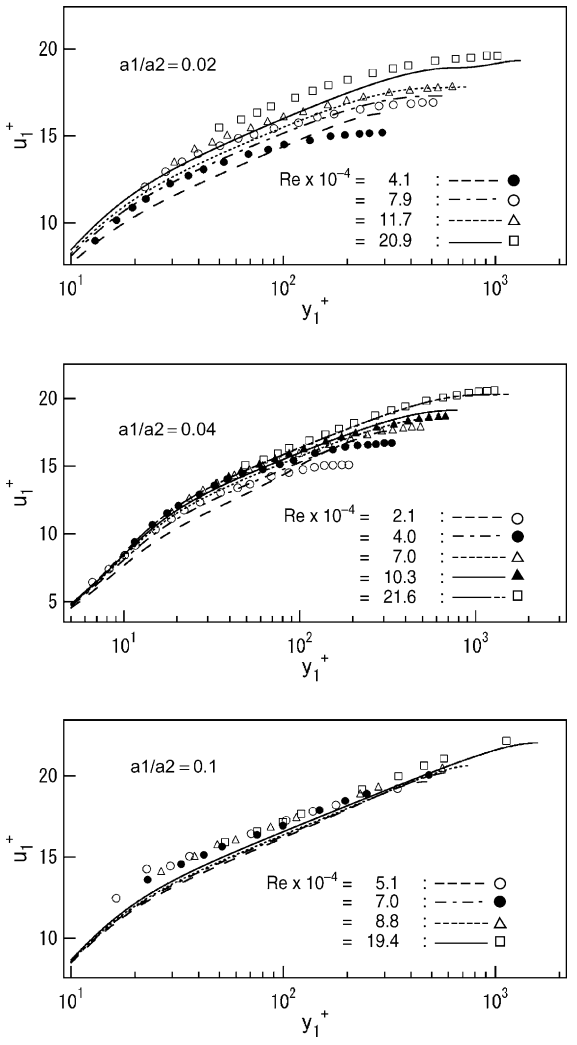

Fig. 6. Comparison of predictive expression for $u^+\{y^+\}$ in the inner region with experimental data of Rehme [12].

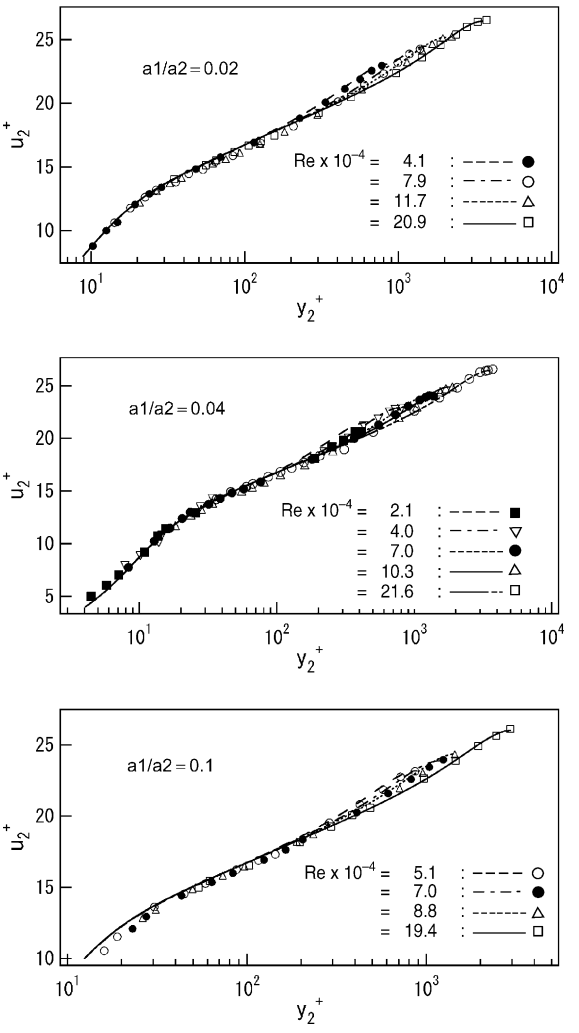

Fig. 7. Comparison of predictive expression for $u^+\{y^+\}$ in the outer region with experimental data of Rehme [12].

of the data. Experimental values for very small aspect ratios might be expected to be uncertain because of the difficulty of obtaining perfect alignment of the inner tube, rod, or wire, and of the likelihood of disturbing the flow by the devices that maintain the alignment. Hence the discrepancies between the predictions and measurements in Fig. 6 may have those explanations in part.

The directly computed values of u_m^+, that is those based on τ_{w1}, as obtained by stepwise integration of the directly computed values of u_{w1}^+ over the cross-section of the annulus, are listed in Table 3 as a function of a_1/a_2 and $a_2^+ - a_1^+$. The corresponding values of the Fanning friction factor, f_{wm}, that is, based on τ_{wm}, are listed in Table 4, and the Reynolds number based on the *hydraulic diameter*, $Re = 2(a_2^+ - a_1^+)u_m^+$, in Table 5. Both the friction factor based on τ_{wm} and the Reynolds number may be seen to be virtually independent of a_1/a_2 except for very small values, whereas u_m^+ varies significantly, as would f_{w1}. The Reynolds number, as defined herein, is independent of the normalizing shear stress on the wall as long as the same one is used for both u_m^+ and $a_2^+ - a_1^+$. Values of u_m^+, f_{wm}, and Re thought to be improbable on the basis of the value of C' for the same condition are shaded in Tables 3–5, and values resulting from uncertain convergence in any respect are omitted.

It was noted in the course of this work that the correlating equation of Danov et al. [2] for a parallel-plate channel, namely,

$$\left(\frac{1}{f}\right)^{1/2} = u_m^+ = 4.165 + \frac{1}{0.436}\ln(b^+) - \frac{155}{b^+} \tag{23}$$

Table 3
Computed values of u_m^+ (based on τ_{w1})

a_1/a_2	$a_2^+ - a_1^+$											
	150	500	800	1000	2000	5000	10,000	20,000	50,000	100,000	200,000	500,000
0.01		10.29	11.20	11.60	12.77							
0.05	9.64	13.04	14.11	14.59	16.00	17.76	19.04					
0.1	10.58	14.21	15.35	15.86	17.37	19.26	20.64	22.00	23.77	25.06		
0.2	11.49	15.25	16.46	17.00	18.60	20.61	22.08	23.52	25.40	26.78	28.09	29.59
0.5	12.25	16.31	17.60	18.17	19.88	22.00	23.57	25.11	27.11	28.58	29.99	31.62
0.8	12.49	16.69	18.01	18.61	20.35	22.54	24.14	25.72	27.77	29.28	30.73	32.43
0.9	12.53	16.77	18.10	18.70	20.46	22.65	24.26	25.85	27.92	29.44	30.90	32.61
0.95	12.55	16.80	18.14	18.74	20.50	22.70	24.32	25.91	27.98	29.51	30.97	32.69
0.99	12.56	16.83	18.17	18.77	20.54	22.74	24.36	25.95	28.03	29.56	31.02	32.75
0.999	12.56	16.83	18.17	18.78	20.54	22.75	24.37	25.96	28.04	29.57	31.04	32.76

Table 4
Computed values of Fanning friction factor ($\times 10^{-3}$) based on the mean shear stress on the walls and the total flow

a_1/a_2	$a_2^+ - a_1^+$											
	150	500	800	1000	2000	5000	10,000	20,000	50,000	100,000	200,000	500,000
0.01		8.013	6.755	6.303	5.201							
0.05	13.73	7.503	6.414	6.000	4.988	4.049	3.521					
0.1	13.26	7.355	6.304	5.903	4.921	4.004	3.485	3.067	2.629	2.365		
0.2	12.77	7.240	6.216	5.826	4.866	3.966	3.456	3.043	2.610	2.348	2.134	1.923
0.5	12.64	7.127	6.123	5.740	4.799	3.915	3.413	3.007	2.579	2.320	2.108	1.896
0.8	12.65	7.080	6.077	5.696	4.760	3.883	3.384	2.981	2.557	2.299	2.088	1.875
0.9	12.66	7.069	6.065	5.684	4.749	3.873	3.376	2.974	2.550	2.293	2.082	1.869
0.95	12.67	7.063	6.060	5.679	4.744	3.869	3.372	2.970	2.547	2.290	2.079	1.866
0.99	12.67	7.059	6.055	5.674	4.740	3.865	3.368	2.967	2.544	2.288	2.077	1.864
0.999	12.68	7.059	6.055	5.673	4.739	3.864	3.368	2.967	2.544	2.287	2.076	1.863

Table 5
Computed values of $Re = 2(a_2^+ - a_1^+)u_m^+$ ($\times 10^{-3}$)

a_1/a_2	$a_2^+ - a_1^+$											
	150	500	800	1000	2000	5000	10,000	20,000	50,000	100,000	200,000	500,000
0.01		10.29	17.92	23.20	51.07							
0.05	2.893	13.04	22.57	29.17	63.99	177.6	380.8					
0.1	3.175	14.21	24.56	31.72	69.49	192.6	412.8	880	2377	5012		
0.2	3.446	15.25	26.34	34.00	74.41	206.1	441.5	941	2540	5356	11240	29590
0.5	3.674	16.31	28.15	36.35	79.50	220.0	471.4	1004	2711	5717	12,000	31,620
0.8	3.746	16.69	28.82	37.21	81.42	225.4	482.8	1029	2777	5857	12,290	32,430
0.9	3.759	16.77	28.96	37.40	81.83	226.5	485.3	1034	2792	5888	12,360	32,610
0.95	3.764	16.80	29.02	37.48	82.01	227.0	486.4	1036	2798	5902	12,390	32,690
0.99	3.768	16.83	29.07	37.54	82.14	227.4	487.2	1038	2803	5912	12,410	32,750
0.999	3.768	16.83	29.08	37.55	82.17	227.5	487.4	1039	2804	5914	12,410	32,760

predicts almost the same numerical value of u_m^+ as the corresponding correlating of Yu et al. [1] for a round tube, namely,

$$\left(\frac{2}{f}\right)^{1/2} = u_m^+ = 3.2 + \frac{1}{0.436}\ln(a^+) - \frac{227}{a^+} + \left(\frac{50}{a^+}\right)^2 \tag{24}$$

if b^+ is simply replaced by $a^+/2$. It was thereupon conjectured on the basis of the values in Table 4 that replacing a^+ by $a_2^+ - a_1^+$ might result in an approximate predictive expression for annuli of all aspect ratios, except possibly at rates of flow very near the minimum for fully developed turbulence, that is in the regime in which the reciprocal term in b^+ in Eq. (23) and the reciprocal

terms in a^+ and $(a^+)^2$ in Eq. (24) contribute significantly. A single term in $(a^+)^{-1}$ with a mean value for the coefficient was introduced to represent approximately the reciprocal terms in both Eqs. (24) and (25), resulting in

$$\left(\frac{2}{f_{wm}}\right)^{1/2} = (u_m^+)_{wm} = 3.2 + \frac{1}{0.436}\ln\{(a_2^+ - a_1^+)_{wm}\} - \frac{275}{(a_2^+ - a_1^+)_{wm}} \quad (25)$$

Eq. (25) may be re-expressed in terms of Re as follows:

$$\left(\frac{2}{f_{wm}}\right)^{1/2} = 1.610 + \frac{1}{0.436}\ln\{Re\} - \frac{550}{Re(f_{wm}/2)^{1/2}} - \frac{1}{0.436}\ln\left\{\left(\frac{2}{f_{wm}}\right)^{1/2}\right\} \quad (26)$$

Eq. (26) is slightly more complicated than Eq. (25) and requires iterative solution for a specified value of Re, but convergence is very rapid, and it has the advantage of being directly comparable with experimental data, which are ordinarily expressed in terms of Re rather than $(a_2^+ - a_1^+)_{wm}$. Eqs. (24) and (25) have the common lower limit of applicability of 150 for a^+ and b^+, respectively, which suggests a lower limit of $(a_2^+ - a_1^+)_{wm} = 300$ for Eq. (25) and of $Re = 10{,}000$ for Eq. (26).

The predictions of Eq. (26) are compared in Fig. 8 with curves representing the computed values of the Fanning friction factor for four values of a_1/a_2, as well as with the experimental values of Lawn and Elliott [5] for three different but intermediate values of a_1/a_2. This discrepancy in the values of a_1/a_2 is not important here because both the experimental data and the curves representing the numerically computed values confirm the conjecture that the parametric dependence on the aspect ratio is negligible when Re based on the hydraulic diameter or when $(a_2^+ - a_1^+)_{wm}$ is chosen as the independent variable. Furthermore, Fig. 8 confirms that Eq. (25) provides a good quantitative prediction of the friction factor for all values of the aspect ratio and Re.

Finally, for illustrative purposes, values of u/u_m computed from the predictive expressions for u^+ and u_m^+ are plotted versus the fractional distance across the channel in Fig. 9 for three or four values of a_1/a_2 and three values of $a_2^+ - a_1^+$. The maximum value of the ratio u_{max}/u_m may be observed to decrease as both a_1/a_2 and $a_2^+ - a_1^+$ increase, while the location of that maximum moves toward the inner wall as a_1/a_2 decreases and $a_2^+ - a_1^+$ increases.

6. Evaluation of results

The new calculated values presented herein are subject to some conjectured functionalities as well as to several empiricisms. One source of arbitrary functionality is the postulate that the structure of the expressions for $(\overline{u'v'})^+$, u^+, and u_m^+ for round tubes and parallel-plate channels is directly applicable for annuli. This postulate appears to be reasonable in that round tubes and parallel-plate channels constitute the bounding cases for annuli as a_1/a_2 varies from 0 to 1. One source of empiricism is the postulate that, with one exception, the same numerical values of the arbitrary coefficients and

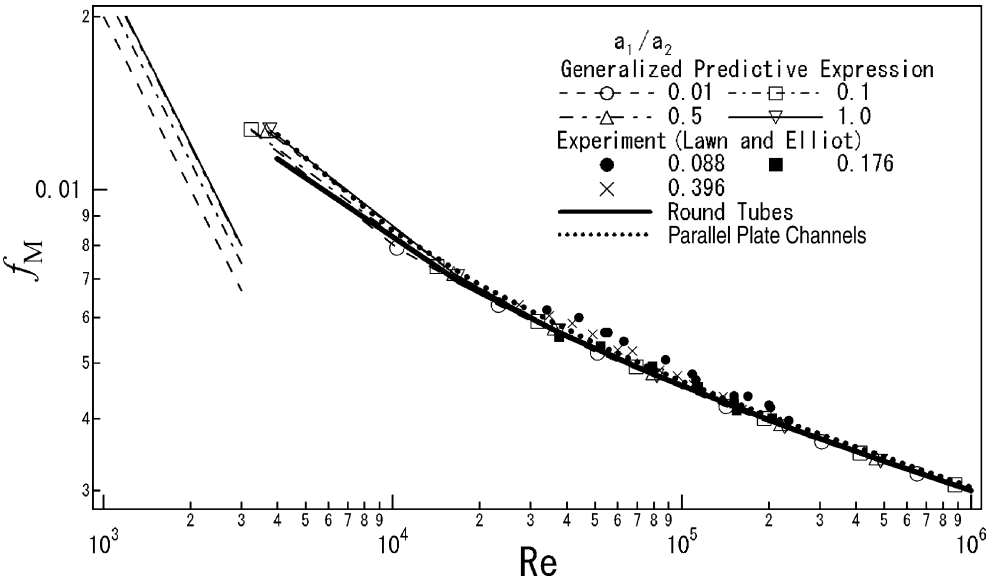

Fig. 8. Comparison of predictive expression for the Fanning friction factor based on the mean shear stress on the walls and the total flow with the computed values and with the experimental data of Lawn and Elliott [3].

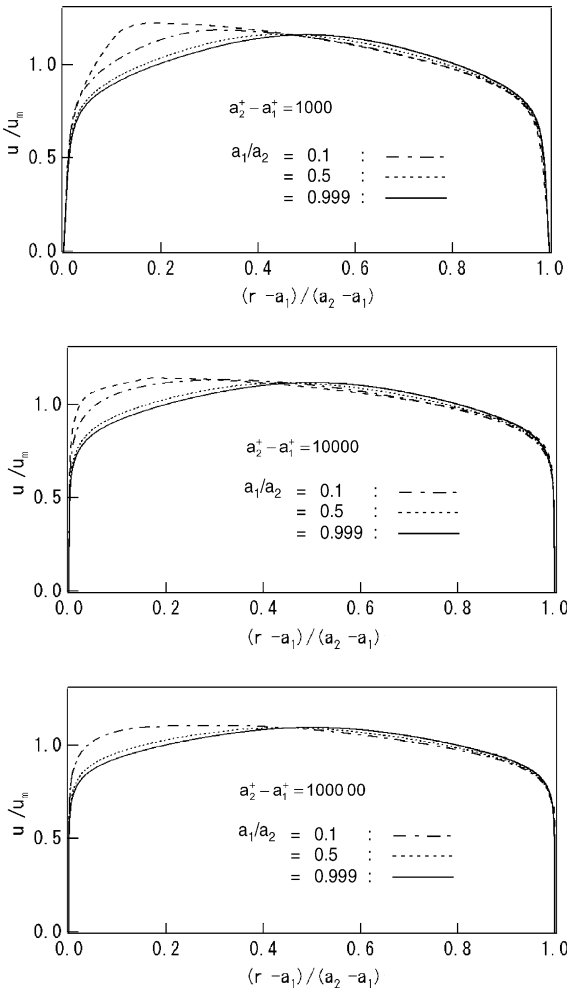

Fig. 9. Predicted relative velocity distribution over the entire annulus.

exponents are applicable. This postulate has the same rationale as the previous one. It should be noted that this same structure and these same coefficients and exponents have previously been shown to predict experimental values of $(\overline{u'v'})^+$, u^+ and u_m^+ almost exactly for both round tubes and parallel-plate channels. The above-mentioned one exception is the allowance of the coefficient C, re-designated as C' for the inner region, to vary with a_1/a_2 and $a_2^+ - a_1^+$ in order to force continuity of the velocity at the location of the maximum in the velocity. This choice, which avoids the need to introduce an additional coefficient, was based primarily on simplicity and does not have a firm rationale. In any event, as discussed previously, it would not be expected to have a significant quantitative effect on $u^+\{y^+\}$ or u_m^+.

Eqs. (8) and (9), which have an experimental basis, are the principal source of empiricism relative to the prior results for round tubes and parallel-plate channels. As a severe test of the numerical uncertainty arising from the use of these two expressions, the calculations for u^+ were repeated using Eq. (10) for both a_0 and $a_{\max}$. The corresponding values of $a_0/a_1 = a_{\max}/a_1$, τ_{w2}/τ_{w1}, and τ_{wM}/τ_{w2} are listed in Table 6 and those of C' in Table 7. They differ significantly from those in Tables 1 and 2 only for very small values of a_1/a_2. Values of $u^+\{y^+\}$ and u_m^+ based on C' from Table 7 were calculated for representative values of a_1/a_2 and $a_2^+ - a_1^+$, but since, as anticipated, they differ negligibly from those based on C' from Table 2, even for small aspect ratios, they are not presented herein. These comparisons appear to indicate that Eqs. (8) and (9) are a negligible source of uncertainty in the computed values and predictive equations. However, they do not confirm or refute a possible dependence of a_0 and $a_{\max}$ on Re. The close correspondence in the values of C' in Tables 2 and 7 suggests that in the interests of simplicity Eq. (10) may be used in conjunction with Eq. (19) to estimate values of C' intermediate to those in Table 7. However, it should not be inferred from the rather minimal error resulting from the use of $(a_{\max} = a_0)_{\text{laminar}}$ to estimate C' that solutions that incorporate this idealization in their basic formulation are necessarily valid.

How is it possible to represent the friction factor for all aspect ratios, as in Eqs. (25) and (26), without an explicit dependence on that quantity? The answer may be found in Table 1 in the minimal variation of τ_{wm}/τ_{w1} from unity as a_1/a_2 varies for a fixed value of $a_2^+ - a_1^+$, and in Table 4 in the corresponding minimal variation in f_{wm}. On the other hand, the choice $(a_2^+ - a_1^+)_{wm}$ as the sole independent variable for the friction factor f_{wm} is an approximation with a purely conjectural basis and is clearly invalid on theoretical grounds for such small values of Re that the deviation from the semi-logarithmic velocity distribution in the buffer and viscous boundary layer must be taken into account. The compensatory terms in Eqs. (25) and (26) simply represent an empirical attempt at a generalized correction for this regime and thereby the extension of their applicability down to the point of attainment of fully turbulent flow.

Table 6
Computed values of $(a_{\max}/a_1 = a_0/a_1)_{\text{laminar}}$, τ_{w2}/τ_{w1} and τ_{wm}/τ_{w2} based on Eq. (10)

a_1/a_2	0.01	0.1	0.2	0.5	0.8	0.9	0.95	0.99	0.999
$(a_{\max}/a_1)_{\text{laminar}}$	32.95	4.637	2.731	1.471	1.123	1.055	1.026	1.005	1.001
τ_{w2}/τ_{w1}	8.22×10^{-2}	0.383	0.543	0.789	0.928	0.965	0.983	0.997	1.000
τ_{wm}/τ_{w2}	1.111	1.146	1.140	1.089	1.034	1.017	1.008	1.002	1.000

Table 7
Compensatory coefficient C' for inner region based on Eq. (10)

a_1/a_2	$a_2^+ - a_1^+$											
	150	500	800	1000	2000	5000	10,000	20,000	50,000	100,000	200,000	500,000
0.01	77.5	25.5	2.36	0.33								
0.05	47.2	3.99	1.18	0.02	−2.94							
0.1	12.4	4.04	2.18	1.45	−0.4	−2.15	−3.14	−4.11	−6.05			
0.2	9.56	4.73	3.65	3.23	2.19	1.19	0.56	−0.02	−0.82	−1.54	−2.47	−4.59
0.5	7.85	5.98	5.58	5.42	5.06	4.67	4.43	4.17	3.76	3.34	2.67	0.96
0.8	7.16	6.55	6.44	6.38	6.27	6.14	6.04	5.93	5.69	5.38	4.83	3.27
0.9	6.98	6.70	6.63	6.61	6.56	6.48	6.43	6.35	6.16	5.89	5.36	3.83
0.95	6.90	6.76	6.73	6.70	6.69	6.64	6.61	6.55	6.37	6.11	5.60	4.08
0.99	6.84	6.81	6.80	6.79	6.79	6.77	6.74	6.69	6.53	6.28	5.78	4.28
0.999	6.825	6.820	6.818	6.817	6.812	6.796	6.773	6.721	6.57	6.32	5.82	4.318

The best rationale for these several arbitrary choices is the excellent agreement of the consequent predictions with experimental data for the time–mean velocity distribution and the friction factor.

The prior numerical solutions for annuli based on eddy-viscosity, mixing-length, or κ–ε models, as well as those that incorporate idealized expressions for $a_{\max}$ and/or a_0, may be dismissed as highly uncertain. Those based on $\overline{u'v'}$, κ–ε–$\overline{u'v'}$, or LES models are free of the empiricism associated with the use of Eqs. (8) and (9), and may actually predict $a_{\max}$ and a_0, but are all subject to considerable uncertainty because of the use of "wall-functions". The trade-off is difficult to evaluate in terms of numerical and functional accuracy, but, in any event, the theoretically structured predictive equations that are the end product of the analysis herein are a huge plus relative to the uncorrelated set of numerical values that result from the prior methods of modeling. Calculated values obtained by means of DNS are essentially free of all empiricism but are still today limited by the magnitude of the required computations and perhaps even intrinsically to values of *Re* only slightly above the minimum for fully developed turbulence. They too produce a set of discrete values differing in structural character from experimental data only by virtue of their imprecision and irregularity, and they do not eliminate the need for correlative equations.

7. Summary and conclusions

On the basis of comparisons with prior experimental data, the computed values presented herein are presumed to be more accurate than any prior ones for annuli with the possible exception of the very limited range of values obtained by DNS. Also, as contrasted with all prior theoretical results, they cover a complete range of flow and of aspect ratio.

The algebraic predictive equations devised herein reproduce almost exactly the computed values of u^+ and $u_m^+ = (2/f)^{1/2}$ for all conditions, and accordingly may be used directly in applications rather than the computed values. The need for additional numerical integrations is thereby eliminated until or unless improved expressions are devised for $a_{\max}$, a_0, and/or $(\overline{u'v'})^+$.

The use of $(a_2^+ - a_1^+)_{wm} = Re(f_{wm}/8)^{1/2}$ as the independent variable was found to eliminate, for all practical purposes, the aspect ratio as a parameter in the algebraic predictive expression for the friction factor, except for flows closely approaching the minimum for fully developed turbulence, and even then to provide a reasonably good numerical approximation.

The predictive expressions for $(\overline{u'v'})^+$, u^+ and u_m^+, as well as the numerically computed values appear to meet the original objective of providing the necessary input for the computation of turbulent convection in annuli.

The greater complexity of the expressions for $(\overline{u'v'})^+$ and u^+ in annuli, as compared with those for round tubes and parallel-plate channels, reflects the greater physical complexity of the flow. Even so, these expressions are not onerous to apply, even with a hand-held calculator.

Eqs. (10) and (21), together with their functional components, as well as Eqs. (25) and (26), are properly designated as *predictive* rather than *correlative* because they were formulated without recourse to the experimental data that they are proposed to represent, or to the computed values, other than in evaluation of the coefficient C', as was necessary for compatibility of the expressions for u^+ for the two regions. Because of the incorporation of theoretically structured asymptotes, they are quite insensitive to the several empirical coefficients and exponents.

References

[1] B. Yu, H. Ozoe, S.W. Churchill, The characteristics of fully developed turbulent convection in a round tube, Chem. Engng. Sci. 56 (2001) 1781–1800.

[2] S.L. Danov, N. Arai, S.W. Churchill, Exact formulations and nearly exact solutions for convection in turbulent flow between parallel plates, Int. J. Heat Mass Transfer 43 (2000) 2767–2777.
[3] F.R. Lorenz, Über turbulente Strömung durch Rohre mit kreisformigen Querschnitt, Mitt. Inst. Strömungs., T.H. Karlsruhe 2 (1932) 26–66.
[4] B. Kjellström, S. Hedberg, On shear stress distributions for flow in smooth or partially rough annuli, Aktiebolagent Atomenergi, Report AE-243, Stockholm, 1966.
[5] C.J. Lawn, C.J. Elliott, Fully developed turbulent flow through concentric annuli, J. Mech. Engng. Sci. 14 (3) (1972) 195–204.
[6] K. Hanjalić, B.E. Launder, A Reynolds stress model of turbulence and its application to thin shear flows, J. Fluid Mech. 52 (4) (1972) 609–638.
[7] H. Kawamura, S. Nakamura, S. Satake, T. Kunugi, Large eddy simulation of turbulent heat transfer in a concentric annulus, Thermal Sci. Engng. 2 (1994) 16–25.
[8] S. Satake, H. Kawamura, Large eddy simulation of turbulent flow in concentric annuli with a thin inner rod, in: F. Durst, N. Kasagi, B.E. Launder, F.W. Schmidt, K. Suzuki, J.H. Whitelaw (Eds.), Turbulent Shear Flows, vol. 9, Springer-Verlag, Berlin, 1993, pp. 259–281.
[9] S.Y. Chung, G.H. Rhee, H.J. Sung, Direct numerical simulation of turbulent concentric annular pipe flow. Part 1: Flow field, Int. J. Heat Fluid Flow 23 (2002) 426–440.
[10] S.W. Churchill, New wine in new bottles; unexpected findings in heat transfer. Part II. A critical examination of turbulent flow and heat transfer in circular annuli, Thermal Sci. Engng. 5 (3) (1997) 1–12.
[11] S.W. Churchill, C. Chan, Turbulent flow in channels in terms of local turbulent shear and normal stresses, AIChE J. 41 (12) (1995) 2513–2521.
[12] S.W. Churchill, New simplified models and formulations for turbulent flow and convection, AIChE J. 43 (5) (1997) 1125–1140.
[13] W.M. Kays, K.T. Leung, Heat transfer in annular passages—hydrodynamically developed turbulent flow with arbitrarily prescribed heat flux, Int. J. Heat Mass Transfer 6 (1963) 537–557.
[14] K. Rehme, Turbulent flow in smooth concentric annuli with small radius ratios, J. Fluid Mech. 64 (1974) 263–287.
[15] M.V. Zagarola, Mean-Flow Scaling of Turbulent Pipe Flow, Ph.D. Thesis, Princeton University, Princeton, NJ, 1996.
[16] A.L. MacLeod, Liquid Turbulence in a Gas–Liquid Absorption System, Ph.D. Thesis, Carnegie Institute of Technology, Pittsburgh, PA, 1951.